Vibration power dissipation in a spring-damper-mass system excited by dry friction

Cui Chao[1], Baiyang Shi[1] and Jian Yang[1,2*]

[1] Department of Mechanical, Materials and Manufacturing Engineering, University of Nottingham Ningbo China, Ningbo 315100, PR China
[2] Centre for Sustainable Energy Technologies (CSET), Faculty of Science and Engineering, University of Nottingham Ningbo China, Ningbo 315100, PR China

[*] Corresponding author, E-mail: jian.yang@nottingham.edu.cn; Tel.: +86-574-88180000 ext 3141

Abstract. This study investigates the vibration transmission and power dissipation behaviour of a mass-spring-damper system mounted on a conveyor belt. Coulomb friction exists between the mass and the belt moving at a constant velocity and acts as the external force for the mass. The steady-state power flow characteristics and system limit cycles are obtained based on numerical integrations. The vibration energy dissipation at the contact interface and by the viscous damper is evaluated and quantified. The vibration transmission is measured by force transmissibility. For the system without the viscous damper, the instantaneous friction power can be positive or negative, depending on the motion characteristics of the mass. For the system with the viscous damper, in the steady-state motion, the vibration energy input caused by the friction can be dissipated by the viscous damper and also by the friction. Furthermore, effects of the magnitude of conveyor belt speed, damping ratio and friction force on the dynamic behaviour of systems are examined, and the power dissipation ratio of the system is analyzed. The results are expected to provide insights into the vibration transmission and suppression design of systems with friction.

Keywords: Vibration Transmission, Power Dissipation, Damped System, Dry friction.

1 Introduction

Friction is a very complex phenomenon and occurs at the interface contacting bodies. It is usually inevitable and plays a significant role in various engineering fields, such as seismology, mechanical engineering and civil engineering. A great number of published studies have revealed rich dynamic behavior of frictional systems [1, 2]. Popp *et al.* [3,4] studied discrete and continuous models with stick-slip phenomena and observed abundant bifurcation and chaotic behaviors. Kruse *et al.* [5] studied the influence of joints on the stability and bifurcation behavior of a friction-induced flutter system. In Ref. [6], both the numerical simulation on low-degree-of-freedom models and the experimental

validation on the real test rigs concerning the friction-induced vibration of systems were implemented.

For a system of a mass placed on conveyor belt, the dry friction has a significant effect on its dynamics. The analysis of the non-linear dynamics for the mass-on-belt system is a fundamental problem for many engineering. Many researchers carried out a number of investigations on the frictional non-linear dynamics [7-9]. However, few studies have considered the energy transmission and dissipation of such system [10]. The vibrational power flow analysis approach is a valuable tool to characterize the dynamic behaviour of complex systems [11]. Royston and Singh [12] examined the energy flow in a hydraulic engine mount system and showed that significant amount of vibration energy can be transmitted through a nonlinear path to a flexible base. Vakakis et al. [13] observed the phenomenon of energy transfer and noted that nonlinear attachment can be used to channel and dissipate the vibration energy of a main structure. Yang et al. [14, 15] developed power flow analysis (PFA) method for nonlinear dynamical systems, which reexamines typical nonlinear systems from a power flow perspective. Recently, the application of PFA to vibration control and vibration energy collection systems are investigated [16-21].

In this paper, the vibration energy flow transmission and dissipation characteristics of nonlinear non-smooth conveyor belt systems are investigated. The Runge-Kutta method is employed to investigate the vibration force transmission and power flow behaviour of systems with dry friction nonlinearity. Effects of the feeding speed, damping ratio and friction force on results are studied.

2 Single-degree of freedom (DOF) Coulomb friction models

Fig. 1(a) shows the mass-on-belt frictional dynamic model, in which a mass block m is placed on the moving belt with a constant speed v_b. The mass is connected to a fixed wall through a viscous damper with damping coefficient c and a linear spring with stiffness coefficient k, connected in parallel. The Coulomb friction exists at the interface between the block and the belt. Fig. 1(b) depicts the Karnopp model [22, 23] used to represent Coulomb friction.

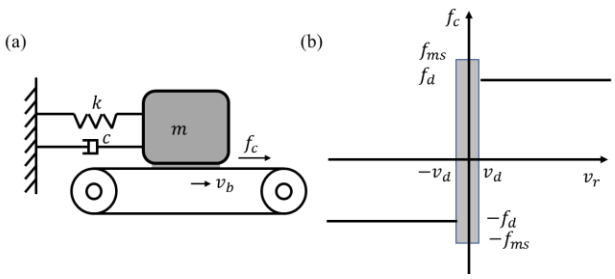

Fig. 1 (a) The spring–mass-damper system on the moving belt, and (b) the Karnopp model with magnitude of the dynamic friction force f_d and maximum static friction force f_{ms}. In (b), v_d is the limiting velocity of the assumed zeros velocity interval $[-v_d, v_d]$ for Karnopp model.

The mass block is subjected to the combined action of the friction, the spring and the damping forces. According to the Newton's second law, the equation of motion of the mass can be expressed as follows:

$$m\ddot{x} + 2c\dot{x} + kx = f_{ex} = f_c \tag{1}$$

where f_{ex} is the external force and f_c is the nonlinear dry friction force acting as the excitation force to the mass. The friction f_c is described by the Karnopp model, written as:

$$f_c = \begin{cases} f_d \mathrm{sgn}(v_r), & \text{if } |v_r| > v_d, \\ f_{ms} \mathrm{sgn}(f_e), & \text{if } |v_r| \le v_d \text{ and } |f_e| \ge f_{ms}, \\ f_e, & \text{if } |v_r| \le v_d \text{ and } |f_e| < f_{ms}. \end{cases} \tag{2}$$

where f_d, f_{ms} and f_e are the dynamic friction force, the maximum static friction force and the resultant external force in tangential direction, respectively; v_d is the boundary velocity of the dead zone for Karnopp model. In this paper, it is assumed that f_d=f_{ms} [24]. When the Karnopp model is used, we have $v_r = v_b - \dot{x}$ and $f_e = kx$ in Eq. (2). Following non-dimensional parameters are defined for parametric studies:

$$\omega_0 = \sqrt{\frac{k}{m}}, \quad \zeta = \frac{c}{2m\omega_0}, \quad X = \frac{x}{l_0}, \quad F_d = \frac{f_d}{kl_0}, \quad V_b = \frac{v_b}{\omega_0 l_0},$$
$$V_d = \frac{v_d}{\omega_0 l_0}, \quad V_r = V_b - X', \quad \tau = \omega_0 t \tag{3}$$

where ω_0 and ζ are the undamped natural frequency and the damping ratio of the system without considering the friction, l_0 and X are the undeformed length of the linear spring and the dimensionless displacement of the mass, F_d is the non-dimensional magnitude of the dynamic dry friction force named magnitude of friction hereafter, V_b, V_d and V_r are the dimensionless velocity of the belt, limiting velocity of the assumed zeros velocity interval in the Karnopp model and relative velocity between the block and the mass, respectively, and τ is the dimensionless time. By using those parameters in Eq. (3), Eq. (1) can be transformed into its non-dimensional form:

$$X'' + 2\zeta X' + X = F_c \tag{4}$$

where F_c is the non-dimensional friction force, and is expressed by

$$F_c = \begin{cases} F_d \mathrm{sgn}(V_r), & \text{if } |V_r| > V_d, \\ F_d \mathrm{sgn}(F_e), & \text{if } |V_r| \le V_d \text{ and } |F_e| \ge F_d, \\ F_e, & \text{if } |V_r| \le V_d \text{ and } |F_e| < F_d. \end{cases} \tag{5}$$

where $F_e = X$ is the non-dimensional resultant force applied to the contacting interface in the tangential direction.

Two cases are considered in this paper: Case *I* considers the absence of the viscous damper (i.e., damping coefficient is set to zero), while Case *II* considers the presence of

the viscous damper. The fourth-order Runge-Kutta method is used for the dynamic analysis to obtain the response and power flow variables.

3 Energy flow and force transmissibility

3.1 Force transmissibility

To evaluate the level of vibration transmission between subsystems of an integrated linear or nonlinear structure, the force transmissibility has been widely employed as indicator [25]. For the current SDOF system with friction, the force transmissibility TR_B can be defined as the ratio between the maximum magnitude of the transmitted force to the wall and the amplitude of the external force:

$$TR_B = \frac{\max(|\Re(F_{tB})|)}{F_{ex}} \tag{6}$$

where F_{tB} represents the non-dimensional transmitted force from mass to the wall. $F_{tB} = X$ is for the system without dampers (Case *I*), while $F_{tB} = X + 2\zeta X'$ is for the system with a damper (Case *II*). For the frictional system without external force excitation, the friction can be treated as the input force of the mass-spring-damper system, so that the F_{ex} in Eq. (6) can be replaced by F_d.

3.2 Time-averaged power flow variables

Pre-multiplying the governing equation (4) by the velocity X', the equation of power balance of the system is obtained:

$$X'X'' + 2\zeta X'X' + X'X = X'F_c(\Delta(X')) \tag{7}$$

Alternatively, it can be written in the following form:

$$\dot{K} + p_{dv} + \dot{U} = P_f \tag{8}$$

where $\dot{K} = X'X''$ and $\dot{U} = X'X$ are the non-dimensional rates of change of system kinetic and potential energies. $P_{dv} = X'X'$ and $P_f = X'F_c(\Delta(X'))$ are dimensionless instantaneous dissipated power and friction related power. In this paper, time-averaged behaviour of power flows is considered. Using an averaging time span of τ_p:

$$\bar{P}_{dv} = \frac{1}{\tau_p}\int_{\tau_i}^{\tau_i+\tau_p} P_{dv}\mathrm{d}\tau = \frac{1}{\tau_p}\int_{\tau_i}^{\tau_i+\tau_p} 2\zeta X'X'\mathrm{d}\tau, \tag{9a}$$

$$\bar{P}_{df} = \frac{1}{\tau_p}\int_{\tau_i}^{\tau_i+\tau_p} \mathrm{H}(-P_f)\mathrm{d}\tau = \frac{1}{\tau_p}\int_{\tau_i}^{\tau_i+\tau_p} \mathrm{H}(-X'F_c(\Delta(X')))\,\mathrm{d}\tau \tag{9b}$$

$$\bar{P}_{f\_in} = \frac{1}{\tau_p}\int_{\tau_i}^{\tau_i+\tau_p} \mathrm{H}(P_f)\mathrm{d}\tau = \frac{1}{\tau_p}\int_{\tau_i}^{\tau_i+\tau_p} \mathrm{H}(X'F_c(\Delta(X')))\,\mathrm{d}\tau \tag{9c}$$

where H() denotes the Heaviside step function, and τ_i is the starting time for averaging. $\bar{P}_{dv}$ denotes the time-averaged dissipated power by the damper, $\bar{P}_{df}$ is the power dissipated by the friction that is converted into heat, and $\bar{P}_{f\_in}$ is the input power by friction. For a periodic response, we have $\bar{P}_{dv} + \bar{P}_{df} = \bar{P}_{f\_in}$ with the averaging time set as one periodic cycle. $R_c = \frac{\bar{P}_{dv}}{\bar{P}_{f\_in}}$ and $R_f = \frac{\bar{P}_{df}}{\bar{P}_{f\_in}}$ are time-averaged power dissipation ratio by the damping and the friction.

4 Results and discussions

This study focuses on the power flow characteristics of system with dry friction contact at the interface. It is assumed that initially at $t = 0$, the mass is placed on the belt such that their velocities are the same. The friction points to the right and forces the block to slide to the right, while the spring and the damping force act against the motion. The non-smoothness of the friction force is reflected by the conditional statement in the algorithm for numerical integrations of the governing equation. Another system parameter is fixed as $V_d = 10^{-3}$. The steady-state responses and the vibration dynamics of the system are of interest here and initial conditions can be set as $X(0) = F_d$, $X'(0) = V_b$.

Figure 2 shows time histories of power dissipation by the friction for Case *I* without the presence of the viscous damper. Based on the given initial conditions, it shows that the steady-state instantaneous total power of the friction can be positive or negative depending on the direction of friction and velocity. When the feeding speed V_b is not greater than the limiting velocity V_d for the Karnopp friction model, the stick phenomenon will occur. When the speed of the conveyor belt is larger, the system exhibits periodic self-excited vibrations. Compared with the classical mass-spring-damper system without conveyor belt, the friction force in case *I* is the energy source when the mass slides on the conveyor, and it provides energy input into this system. Over a cycle of periodic oscillation, the total energy input by the friction equals to the energy dissipated by the friction, indicating that the work done by sliding friction on the block in case *I* is dissipated by itself.

Figure 3 shows the steady-state limit oscillations of the system with consideration of the viscous damper. Fig. 3(a) presents effects of different damping ratios on limit cycles, suggesting that a larger damping ratio correspond to a smaller limit cycle. It also shows that the conveyor belt speed has little influence on the magnitude of the limit cycle. It demonstrates that case *II* system is stable and has self-excited periodic vibrations in the steady state.

Figure 4 presents the instantaneous power flow of the system considered in case *II* with the viscous damper. As depicted in Fig. 4(a) and (d), when the magnitude of friction F_d increases from 0.02 to 0.04, the power dissipation by the viscous damping is not affected while the amplitude of the friction power flow increases. As shown in Fig. 4(b) and (e), by changing the value of the conveyor belt speed V_b from 0.01 to 0.1, the figure shows only phase changes in the damping dissipated energy and the frictional power flows. From Fig. 4(c) and (f), as the damping ratio ζ increases from 0.01 to 0.03, amplitudes of the power flow magnitude of the viscous damper and the friction are further

reduced. By a comparison of case *I*, the friction force also provides power input into the system but the positive part of the frictional power flow is slightly larger than the negative part through calculation. The reason is that the value of power dissipation by the viscous damper is small being smaller than 10^{-11}. In contrast, the order of magnitude of frictional power flow is larger, 10^{-6} in Fig. 4(d), (e) and (f).

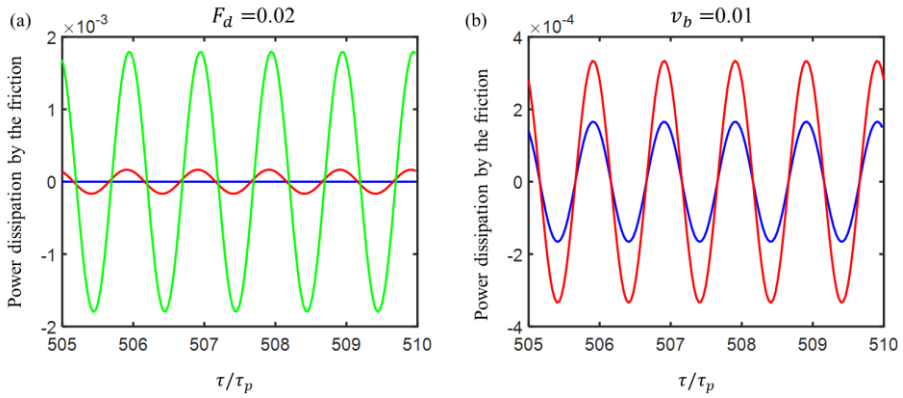

Fig. 2. Time histories of instantaneous power dissipation by the friction for case *I* in the steady state. In (a), the blue, red and green lines are the quantities for $V_b = 0.001, 0.01$ and 0.1 with a consistent $F_d = 0.02$, respectively. In (b), the blue and red lines are the characteristic for $F_d = 0.02$ and 0.04 with a consistent $V_b = 0.01$, respectively. Initial conditions: X(0)=F_d, X′(0)=V_b.

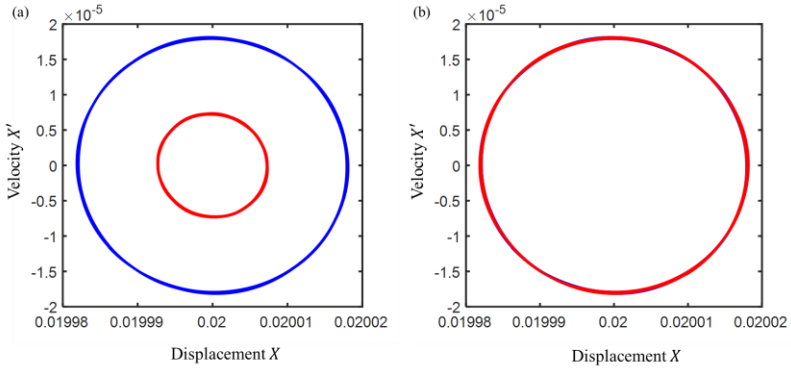

Fig. 3. Limit cycles on steady-state response for case *II* (the effect of the damper is considered). In (a), the blue and red lines are characteristics for $\zeta = 0.01$ and 0.03 with consistent parameters of $F_d = 0.02$, $V_b = 0.01$. In (b), the blue and red lines are the characteristic for $V_b = 0.01$ and 0.1 with consistent parameters of $F_d = 0.02$, $\zeta = 0.01$. Initial conditions: X(0)=F_d, X′(0)=V_b.

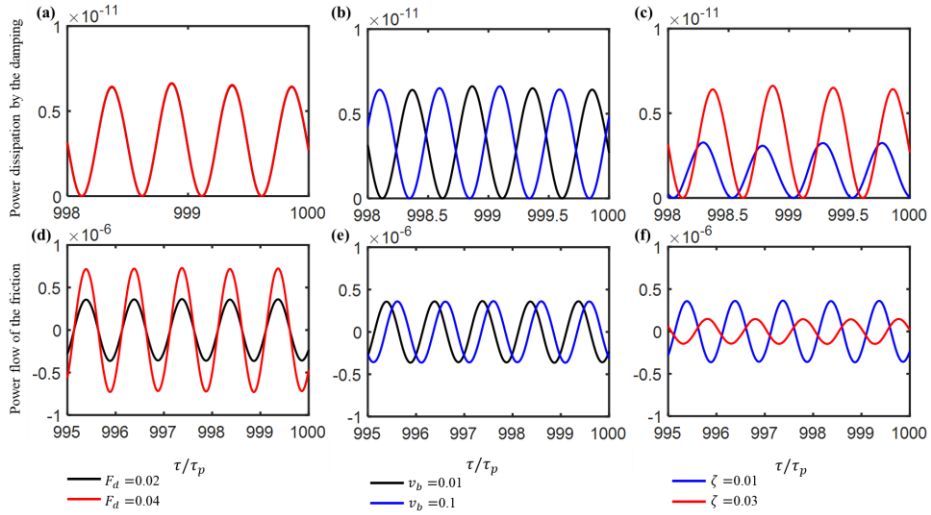

Fig. 4. Instantaneous power flow quantities of system on steady-state motion for case *II* (the effect of the viscous damper is considered). In (a) and (d), the black and red lines are characteristics for $F_d = 0.02$ and 0.04 with consistent parameters of $\zeta = 0.01$ and $V_b = 0.01$. In (b) and (e), the black and blue lines are characteristics for $V_b = 0.01$ and 0.1 with consistent parameters of $F_d = 0.02$ and $\zeta = 0.01$. In (c) and (f), the blue and red lines are characteristics for $\zeta = 0.01$ and 0.03 with consistent parameters of $F_d = 0.02$ and $V_b = 0.01$. (a), (b) and (c) are the instantaneous power dissipation characteristics by the viscous damping. (d), (e) and (f) are power flow quantities of the friction force. Initial conditions: X(0)=F_d, X'(0)=V_b.

The energy dissipation is further investigated to reveal dynamics of the system. Fig. 5(a) and (b) shows the effects of frictional contact on the power flow behavior of the system in the steady-state motion. In Fig. 5(a), the power dissipation ratio by the viscous damper R_c, decreases significantly with the increase of the magnitude of the friction from 0.02 to 0.04, and increases slightly with the damping ratio from 0.01 to 0.03. When the feeding speed from the belt increases to 0.1, the figure shows little change in power flow quantities. In comparison, it is also found that most of the power is dissipated by the friction, about 99.99%. Which is consist with findings in Fig. 4 that the magnitude of the power dissipation by the damper is much smaller than the frictional dissipated power.

In Fig. 6, as the damping ratio ζ of the viscous damper equals zero (i.e., case *I*), effects of the magnitude of dry friction F_d and conveyer belt speed V_b on the force transmissibility TR_B are obtained. It can be found that TR_B decreases with friction force increase from 0.02 to 0.04 due to frictional resistance. On the other hand, TR_B increases as the belt speed V_b increases from 0.01 to 0.1. For case *II* considering the viscous damper, changes of the magnitude of friction force, damping ratio and feeding velocity can hardly affect the value of TR_B because of small change of the transmitted force F_{tB}. Fig. 6 also shows that the force transmission to the wall has a downward trend with the increase of the damping ratio, resulting from smaller limit cycles in Fig. 3(a). Compared

with the effects of the belt speed, variations in the level of dry friction and damping have a relatively large effect on the force transmissibility.

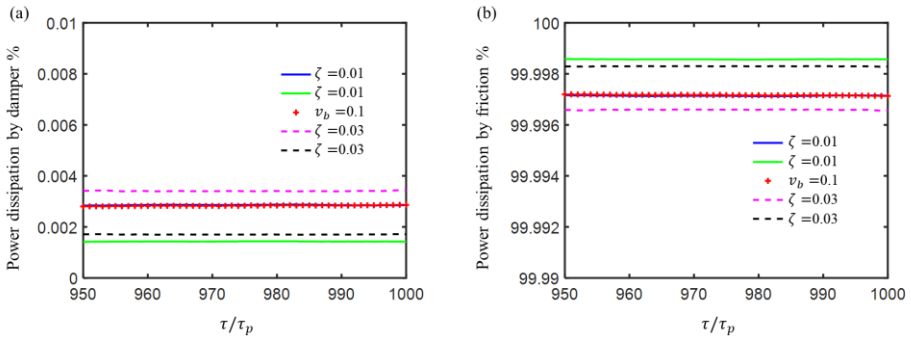

Fig. 5. Effects of the magnitude of friction F_d, damping coefficient ζ and conveyor belt speed V_b on the time-averaged power dissipation ratio (a) by the damper R_c of the system and (b) by the friction R_f. The blue and green lines are characteristics of $V_b = 0.01$, $F_d = 0.02$ and 0.04. The solid lines show the time-averaged power dissipation ratio of $\zeta = 0.01$ and the dash lines are for $\zeta = 0.03$. The red symbol indicates the case for $V_b = 0.1$ of $\zeta = 0.01$ and $F_d = 0.02$. Initial conditions: X(0)=F_d, X′(0)=V_b.

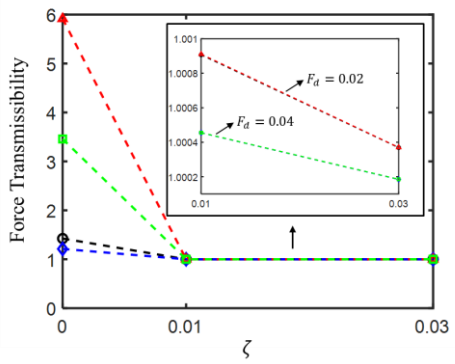

Fig. 6. Force transmissibility of system versus damping ratio ζ in steady-state motion. The black and blue lines are the characteristics of $V_b = 0.01$ for $F_d = 0.02$ and 0.04. The red and green lines are the characteristics of $V_b = 0.1$ for $F_d = 0.02$ and 0.04. Initial conditions: X(0)=F_d, X′(0)=V_b.

5 Conclusions

This study investigated the power flow characteristic of a mass-spring-damper with a mass placed on a belt moving with constant velocity. Coulomb friction with Karnopp model is considered at the mass-belt interface. Time histories of the power flow quantities are obtained for two different cases with and without considering the viscous damper. The net power flow is zero when the viscous damping is ignored, that is, the

work done by friction is dissipated by itself. When the damping is considered, the power flow magnitude of the friction is suppressed with the increase of the damping ratio ζ (which is the relative value between damping force and critical damping force). The magnitude of the friction has significant influence on frictional power flow but little effect on the damper's power flow. It is also found that the feeding speed of the system influences the phase of the steady-state response. By analyzing the time-averaged power dissipation ratio of the system, it is found that most of the power is dissipated by the friction not by the viscous damper. It is also shown that the force transmissibility of the system is mainly affected by the friction force and damping coefficient. These findings improve the understanding of the vibration transmission and suppression design of frictional systems.

Acknowledgement

This work was supported by National Natural Science Foundation of China under Grant number 12172185 and by the Zhejiang Provincial Natural Science Foundation under Grant number LY22A020006.

References

1. R.A. Ibrahim, Friction-induced vibration, chatter, squeal, and chaos, Part II: dynamic and modeling, Appl. Mech. Rev. 47 (1994) 227e253.
2. J. McMillan, A non-linear friction model for self-excited vibrations, J. Sound Vib. 205 (1997) 323e335.
3. Popp, K., Hinrichs, N., Oestreich, M.: Dynamical behaviour of a friction oscillator with simultaneous self and external excitation. Sadhana 20(2–4), 627–654 (1995)
4. Popp,K., Stelter,P.:Stick–slip vibrationsandchaos.Philos.Trans. R. Soc. Lond. Ser. A 332(1624), 89–105 (1990)
5. Kruse, S., Tiedemann, M., Zeumer, B., Reuss, P., Hetzler, H., Hoffmann, N.: The influence of joints on friction induced vibration in brake squeal. J. Sound Vib. 340, 239–252 (2015)
6. Wang, X.C., Huang, B., Wang, R.L., Mo, J.L., Ouyang, H.:Friction-induced stick-slip vibration and its experimental validation. Mech. Syst. Signal Process. 142, 106705 (2020)
7. A. J. MCMILLAN 1997 Journal of Sound and Vibration 205, 323-335. A non-linear friction model for self-excited vibrations.
8. N. HINRICHS, M. OESTREICH and K. POPP 1997 Journal of Chaos, Solitons and Fractals 8, 535-558. Dynamics of oscillators with impact and friction.
9. J. M. BALTHAZAR, J. R. CAMPANHA, H. I., WEBER and D. T. MOOK 1999 Mathematical Applications in Engineering' 24 (B. I. Cheshankov and M. D. Todorov, editors), 9-15. So"a: Heron Press. Some remarks on the numerical simulations of ideal and non-ideal self-excited vibrations.
10. Do N, Ferri AA. Energy transfer and dissipation in a three-degree-of-freedom system with stribeck friction. In: Proceedings of the ASME international mechanical engineering congress and exposition; 2005. p. 195–204.

11.Goyder, H.G.D., White, R.G.: Vibrational power flow from machines into built-up structures. J. Sound Vib. 68, 59–117 (1980)
12.Royston, T.J., Singh, R.: Vibratory power flow through a nonlinear path into a resonant receiver. J. Acoust. Soc. Am. 101, 2059–2069 (1997)
13.Vakakis, A.F., Gendelman, O.V., Bergman, L.A., McFarland, D.M., Kerschen, G., Lee, Y.S.: Nonlinear Targeted Energy Transfer in Mechanical and Structural Systems. Springer, New York (2008)
14.Yang, J.: Power Flow Analysis of Nonlinear Dynamical Systems, PhD thesis, University of outhampton, Southampton (2013)
15.Yang, J., Xiong, Y.P., Xing, J.T.: Dynamics and power flow behaviour of a nonlinear vibration isolation system with a negative stiffness mechanism. J. Sound Vib. 332, 167–183 (2013)
16.Yang J, Shi B, Rudd C. On vibration transmission between interactive oscillators with nonlinear coupling interface. Int J Mech Sci 2018;137:238–51.
17.Yang J, Jiang JZ, Neild SA. Dynamic analysis and performance evaluation of nonlinear inerter-based vibration isolators. Nonlinear Dyn 2019;99:1823–39.
18.Shi B, Yang J, Rudd C. On vibration transmission in oscillating systems incorporating bilinear stiffness and damping elements. Int J Mech Sci 2019;150: 458–70.
19.Dai W, Yang J, Shi B. Vibration transmission and power flow in impact oscillators with linear and nonlinear constraints. Int J Mech Sci 2020;168:105234.
20.Dong Z, Shi B, Yang J, Li T. Suppression of vibration transmission in coupled systems with an inerter-based nonlinear joint. Nonlinear Dyn 2021. https://doi.org/10.1007/s11071-021-06847-9.
21.Dai W, Yang J. Vibration transmission and energy flow of impact oscillators with nonlinear motion constraints created by diamond-shaped linkage mechanism. Int J Mech Sci 2021;194:106212.
22.Karnopp D. Computer Simulation of Stick-Slip Friction in Mechanical Dynamic Systems. Journal of Dynamic Systems, Measurement, and Control. 1985;107(1):100-103.
23.Olsson H. Control systems with friction. Doctoral thesis. Department of Automatic Control. Lund Institute of Technology; 1996.
24.Dai, W., Yang, J., & Wiercigroch, M. (2022). Vibration energy flow transmission in systems with Coulomb friction. International Journal of Mechanical Sciences, 214, 106932.
25.Xiong YP, Xing JT, Price WG. A general linear mathematical model of power flow analysis and control for integrated structure-control systems. J Sound Vib 2003.